THE EFFECT OF FORWARD SPEED ON NONLINEAR SHIP MOTION RESPONSES

Olgun Guven Hizir[1], Zhiming Yuan[1], Atilla Incecik[1], Osman Turan[1]

1. *Department of Naval Architecture, Ocean and Marine Engineering, University of Strathclyde, Glasgow, UK*, olgun.hizir@strath.ac.uk

ABSTRACT

Time-domain nonlinear vertical motion response of the S-175 containership advancing in head sea condition in large amplitude waves are analysed and compared with the experimental results provided in the literature. The boundary value problem is solved by linear 3D Rankine source panel method with sources distributed on the ship surface, free surface and control surfaces. Nonlinear fluid forces, which arise from nonlinear restoring and Froude-Kylov forces, are calculated over the instantaneous wetted portion of the ship hull. Radiation forces are kept as linear and presented in terms of impulse response functions using convolution integrals. In large amplitude waves, nonlinear motion responses are identified and presented in terms of transfer functions. The numerical results are well agreed with the experimental results and show a significant non-linear behaviour with the increase in the wave slope. Validation of the in-house developed code is performed and showed good agreement with the experimental results in the large amplitude waves.

Keywords: Time-Domain, Rankine Source Method, Nonlinear Vertical Motions, Forward Speed Influence.

1 INTRODUCTION

The accurate prediction of the seakeeping behaviour of ships in severe sea states has been a high important subject for ship designers and operators. With the developments in the computer technology in the 70's various 2D and 3D frequency-domain approaches were developed and applied in the ship motion and load calculations. Mainly, the problem in the calculation of the forward speed influence on the hydrodynamic forces is attributed to the complex integration of the Green's functions near to the free surface level. In the recent developments, in order to overcome the difficulties in the integration of Green sources at forward speed problems, Rankine Source (RS) method is developed where the free-surface in the vicinity of the ship is discretized with planar elements for the Boundary Value Problem (BVP) solution.

In the present study, a 3D non-linear time domain analysis was performed for the S-175 container ship in various forward speed cases in order to investigate the motion responses of the hull in large amplitude waves using the rigid body approach. The frequency-domain hydrodynamic coefficients are obtained from in-house developed 3D Boundary Element Method (BEM) MHydro program and fed into in-house developed Large Amplitude Response (LARes) program which solves non-linear time-domain motion responses in large amplitude waves.

Mainly, forward speed ship motion problems can be solved using Green's functions by two different techniques which are named to be the Approximate Forward Speed (AFS) and the Exact Forward Speed (EFS) methods. In the AFS method, the BVP is solved with zero speed Green's functions and then forward speed corrections are applied to the hydrodynamic coefficients. This method is known as the Pulsating Source (PS) method and is widely applied in seakeeping programs. In the EFS method, the exact forward speed Green sources are used

to solve forward speed BVP. This method is known as the Translating-Pulsating Source (TPS)method. The PS method has a deficiency which fails to satisfy the forward speed Free Surface Boundary Condition (FSBC) when the oscillating frequency is low and ship speed is high (Inglis and Price, 1981a). TPS method has more accurate formulation in handling the forward speed effects. However, forward speed boundary conditions are hard to satisfy and are computationally expensive. Due to the high oscillatory nature of the Green's functions near to the free surface, small step sizes are needed in the numerical integration which results in a high computational time (Ba and Guilbaud, 1995).

Chang (1977) initiated the first successful application of the TPS method on a Series 60 hull form using 3D panels and observed a better agreement with the experimental data compared to the PS method, except the roll and pitch damping coefficients. Inglis and Price (1981b) used the TPS method to predict hydrodynamic coefficients of a Series 60 hull form advancing with a constant forward speed using a 3D panel method. The authors found better agreement with the experimental data compared to the PS method, but the method over-predicted the pressures around the stern area of the ship due to the lack of viscous forces and artificial stern wave damping. Wu and Taylor (1990) studied on the PS method to calculate hydrodynamic forces on a body oscillating and translating with low forward speed using the perturbation series in terms of forward speed. They revealed that forward speed correction can be performed using perturbation series of the potential in terms of forward speed. Ba and Guilbaud (1995) worked on the TPS method on the integration of the unsteady Green's functions and used Kelvin singularities to achieve fast and accurate results. Their method was not dependent on the frequency and speed parameters. Chapchap et al. (2011) compared the TPS and PS method using 3D panels on S-175 containership for a high forward speed case (Fn=0.275) and they found that heave Response Amplitude Operator (RAO) demonstrated good agreement between both of the methods. However, the TPS method provided larger responses in the pitch RAO around the resonance area due to the under-prediction of the pitch damping coefficients compared to the PS method.

It is observed that the former researches on the forward speed problem are based on Green function that satisfies the Kelvin free surface condition, as well as the radiation condition. It is an effective method for the zero forward problems, but if the vessel is travelling with forward speed, this method still has some limitations. Firstly, it could not account for the near-field flow condition. Secondly, it is impossible for the Green function to account for the effects of the unsteady flow on the steady potential. In the present study, the Rankine source approach will be applied, which uses a very simple Green function in the boundary integral formulation. This method requires the sources distributed not only on the body surface, but also on the free surface and control surface. Therefore, a flexible choice of free-surface conditions can be realized in these methods. The coupled behaviour between steady and unsteady wave potential could be expressed in a direct formula. Meanwhile, the nonlinearity on the free surface could also be added in the boundary condition.

The Rankine source approach is used by investigators from MIT (Kring, 1994; Nakos and Sclavounos, 1990; Scalvounos and Nakos, 1988) which is applied to the BVP to model steady and unsteady waves as a ship moves in waves. An analysis technique developed by Sclavounos and Nakos (Scalvounos and Nakos, 1988) for the propagation of gravity waves on a panelized free surface showed that a Rankine method could adequately predict the ship wave patterns and forces. Their work led to the development of a frequency-domain formulation for ship motions with a consistent linearization based upon the double-body steady flow model which assumes small and moderate Froude numbers. This model was extended to the time domain by Kring (1994) who also proposed a physically rational set of Kutta conditions at a ship's transom stern. However, there are still some limitations for the extensive use of the Rankine source approach. A very popular radiation condition for the forward speed problem, which is so-called upstream radiation condition, was proposed by Nakos (Nakos, 1990). The free surface was truncated at some upstream points, and a quiescent boundary condition was imposed at these points to ensure the consistency of the upstream truncation of the free surface. Another method to deal with the radiation condition is to move the source points on the free surface at some distance downstream (Jensen et al., 1986). The results from these two methods show very good agreement with published experimental data when the parameter τ ($\tau = u\omega/g$) is greater than 0.25, since they are both based on the assumption that there is no scattered wave travelling ahead of the vessel. However, when the forward speed of the vessel

is very low, τ will be smaller than 0.25, the scattered waves could travel ahead of the vessel, and these traditional radiation conditions could no longer be valid. Das and Cheung (2012a, c) corrected the Sommerfeld radiation condition by taking into account the Doppler shift of the scattered waves at the control surface that truncates the infinite fluid domain. They compared their results with the experimental data, and good agreement was achieved. Yuan et al.(2014) applied Das and Cheung's radiation condition to a Wigley III hull advancing in waves, and very good agreement had been achieved between their predictions and measurements.

Linear frequency-domain calculation of ship motions is an industrial standard due to its well establishment and low computational expense. However, linear frequency domain solutions are valid only for linear small oscillatory responses. Therefore, when the vessel is subjected to large amplitude waves and sinusoidal response characteristics are violated and one needs to calculate responses with non-linear time-domain approaches.

Mainly, time-domain modelling can be separated into two approaches namely: Direct time-domain and hybrid time domain. In direct time domain approach transient Green functions are used and motion equations resulting from the Newton's law are integrated in each time step, but in the hybrid time-domain approach once the frequency domain BVP is solved then the resultant hydrodynamic data is processed with Fourier transforms and implemented via using impulse-response functions to the time-domain motion equations. Cummins (1962) used the latter approach in order to solve time domain responses. In this study hybrid time-domain approach is used because it is simple and computationally less expensive compared to the direct time-domain approach. In hybrid time-domain approach, once the hydrodynamic coefficients are solved, various time-domain simulations can be performed in a short-time. The time requirement in order to solve the BVP problem is highly dependent on the panel number and the frequency range in the calculations. In the current study one non-linear time-domain simulation takes around 2% of the total time required for the frequency domain calculation and this shows the advantage of hybrid time-domain method over direct time-domain method.

Recently, many researchers used Cummins approach to solve large amplitude time-domain motions due to its effectiveness and accuracy in ship responses. Fonseca and Soares (1998) assessed large vertical motions and loads in time domain and revealed that vertical motions are smaller than the linear responses in large amplitude waves while the vertical shear force and bending moment at sagging position are larger than the linear calculations. Non-linear results were closer to the experiments when compared with linear results in large amplitude waves. Watanabe and Guedes Soares (1999) performed a benchmark study of different non-linear time domain codes with rigid and elastic hull approach to assess the effects of large amplitude waves on the internal loads on the ship. They found that the elastic behaviour of the hull play a significant role in derived loads while the agreement of numerical and experimental is getting worse in large wave steepness. Tuitman (2010) used 3-D approach and solved time-domain equations combining with hydro-elastic formulation in large amplitude motions. The author emphasised the importance of the slamming and whipping responses in large amplitude waves. Bruzzone et al. (2011) solved nonlinear large amplitude ship motions using 2-D and 3-D approach with Rankine sources. In 2-D strip theory Rankine source application provided better results in heave motions while 3-D approach performed better in pitch motions compared to the experimental results. Song et al. (2011) assessed the effects of large amplitude motions and loads using 3D Rankine panel method. Motion and load calculations were performed on a modern 6500 TEU container ship for a range of incident wave angles and wave heights. In their study, numerical calculations were performed for low forward speed due to the limitation of the double-body basis flow assumption. The authors noted that, in oblique waves and at low frequencies, spring-damper forces had a significant importance in the motion responses.

In this study three-dimensional non-linear time domain analysis was performed for the S-175 container ship in various forward speed cases in order to investigate the motion responses of the hull in large amplitude waves using rigid body approach. Linear motion Response Amplitude Operator (RAO)'s obtained by the MHydro program are compared with the experimental study performed by Fonseca and Soares (2004) in order to validate the small amplitude motion responses. Moreover, the non-linear results are compared with the ITTC (2010) experiments with respect to the increasing wave slope around the resonant frequency in various forward speed cases. This study emphasizes the importance of the modelling of the forward speed effects on the non-linear motion responses in large amplitude waves. In order to fulfil the aim of the study, four different forward speed cases (Fn=0.15, 0.20, 0.25, 0.275) are compared relatively to each other

with respect to the increasing wave slope. In ISSC (2009) nonlinear seakeeping methods were classified into six different levels with respect to their nonlinearity assumptions implemented in the numerical simulations from the linear methods to the fully nonlinear methods. In the current study, the Froude-Krylov (F-K) nonlinear approach is implemented which corresponds to the level 2 using the taxonomy given by the ISSC. The frequency domain hydrodynamic coefficients which are obtained by using the in-house developed Mhydro code are processed using the in-house developed LARes Level 2 (L2) code.In order to calculate nonlinear hydrodynamic forces accurately in numerical calculations F-K and restoring forces have been calculated with respect to the instantaneous exact wetted area of the body, however; radiation and diffraction forces are kept as linear and calculated at the mean position of the body. Radiation forces in time-domain are represented with the convolution integral of the memory effect of radiating waves due to their dependency in the history of the fluid motion.

2 THEORETICAL BACKGROUND

2.1 Frequency-domain

In this section, frequency-domain solution of the forward speed BVP is summarised. The present study uses a novel Rankine source approach which was originally developed by Yuan (2014) in order to solve BVP using the EFS method.

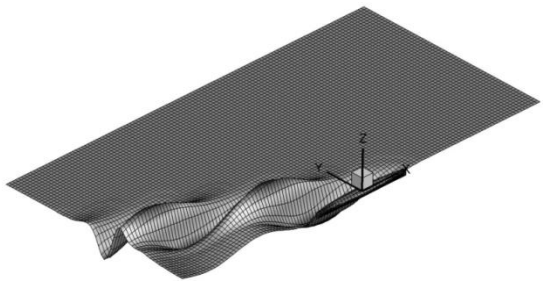

Figure 1: An example vessel and coordinate system

Figure 1 shows a vessel travelling with a constant forward speed in a Cartesian coordinate system which is moving together with the body. In the current study, the hydrodynamic frame axis origin translates with a constant velocity and constant heading as the ship advances and lies on the undisturbed free surface. The z axis points vertically upwards and passes through the Centre of Gravity (CoG) of the ship and the x axis points in the direction in which the ship is heading. Based on the assumption that the surrounding fluid is inviscid and incompressible, and that the motion is irrotational, the total velocity potential exists which satisfies the Laplace equation in the whole fluid domain. For linearization, the so-called Neumann-Kelvin condition will be applied to the free surface boundary condition, and the boundary value problem can be descripted as:

$$\nabla^2 \varphi_j = 0 \qquad \text{in the fluid domain} \tag{1}$$

$$-\omega_e^2 \varphi_j - 2i\omega_e u_0 \frac{\partial \varphi_j}{\partial x} + u_0^2 \frac{\partial^2 \varphi_j}{\partial x^2} + g \frac{\partial \varphi_j}{\partial z} = 0 \qquad \text{on the undisturbed free surface } S_f \tag{2}$$

$$\frac{\partial \varphi_j}{\partial n} = \begin{cases} -i\omega_e n_j + u_0 m_j, \; j = 1,2,...,6 \\ -\dfrac{\partial \varphi_0}{\partial n}, \; j = 7 \end{cases} \qquad \text{on the mean wetted part of the body surface } S_b \tag{3}$$

The radiation condition at infinity is also imposed to complete the boundary value problem, which can be found in Yuan (2014). In Eq. (1) to (3), φ_j is the unsteady perturbation potential, φ_0 is the incident wave potential. The generalized normal vectors are defined as:

$$n_j = \begin{cases} \vec{n}, \; j = 1,2,3 \\ \vec{x} \times \vec{n}, \; j = 4,5,6 \end{cases} \tag{4}$$

and $\vec{n} = (n_1, n_2, n_3)$ is the unit normal vector directed inward on body surface S_b, $\vec{x} = (x, y, z)$ is the position vector on S_b. The m_j denotes the *j-th* component of the so-called *m*-term , and in the present study, it can be expressed as

$$\begin{aligned}(m_1, m_2, m_3) &= (0, 0, 0)\\ (m_4, m_5, m_6) &= (0, n_3, -n_2)\end{aligned} \tag{5}$$

Once the unknown potential φ_j are solved, the steady pressure and the time-harmonic pressure can be obtained from Bernoulli's equation:

$$p_j = -\rho\left[i\omega_e \varphi_j + \nabla(\varphi_s + u_0 x)\cdot\nabla\varphi_j \right] \qquad j=0, 1,\ldots, 7 \tag{6}$$

The hydrodynamic force produced by the oscillatory motions of the vessel in the six degrees of freedom can be derived from the radiation potential as:

$$F_i^D = \sum_{j=1}^{6} \iint_{S_b} p_j n_i dS \cdot \eta_j = \sum_{j=1}^{6} \left[\omega_e^2 \mu_{ij} + i\omega_e \lambda_{ij} \right] \eta_j \qquad j=0, 1,2,\ldots, 6 \tag{7}$$

where μ_{ij} and λ_{ij} are the added mass and damping coefficients matrices respectively, which can be written as:

$$\mu_{ij} = \frac{1}{\omega_e{}^2} \iint_{S_b} \left(u_0 \frac{\partial \varphi_{Rj}}{\partial x} - \omega_e \varphi_{Ij} \right) n_i ds \qquad j=0, 1,2,\ldots, 6 \tag{8}$$

$$\lambda_{ij} = -\frac{1}{\omega_e} \iint_{S_b} \left(u_0 \frac{\partial \varphi_{Ij}}{\partial x} + \omega_e \varphi_{Rj} \right) n_i ds \qquad j=0, 1,2,\ldots, 6 \tag{9}$$

where φ_{Rj} is the real part of *j-th* potential, and φ_{Ij} is the imaginary part. The wave excitation force can be obtained by the integration of incident and diffraction pressure as:

$$F_i^{ext} = \iint_{S_b} (p_0 + p_7) n_i dS \cdot \eta_0 \tag{10}$$

2.2 Time-domain

In this section, large amplitude motion simulations of rigid bodies in a time stepping procedure will be explained. In large amplitude motion simulations calculation of wetted panels in a time instance has crucial importance. LARes L2 uses constant panel mesh, but evaluates the instantaneous wave profile and the wetted portion of the ship at each time step. Each panel's centre position is checked whether it is under wave profile or not and if it is under the wave profile it is concerned as wet otherwise dry. Using the instantaneous wetted panels incident wave forces and hydrostatic forces are evaluated at each time instant. Diffraction and radiation forces are evaluated with respect to the mean sea surface at initial position of the hull. Diffraction forces are kept as linear and obtained from frequency domain solution. Radiation forces are calculated from the convolution part of memory effects of radiating water. In time domain solution approach, motion equations are written applying impulse theory (Cummins, 1962) and the equation is stated as:

$$\begin{aligned}\left[M_{jk}^h + A_{jk}^h(\infty)\right]\cdot\ddot{\xi}_k(t) + B_{jk}^h(\infty)\cdot\dot{\xi}_k(t) + \int_0^t K_{jk}^h(t-\tau)\cdot\dot{\xi}_k(\tau)d\tau + C_{jk}^h\cdot\xi_k(t)\\ = F_j^I(t) + F_j^D(t)\end{aligned} \qquad \text{j,k=3\&5} \tag{11}$$

where j,k=3&5 subscripts stand for the heave and pitch motion modes respectively. The left side of the equation gives the fluid reaction forces and inertial forces whilst the right hand side of the equation gives the excitation forces in the time domain. In the Equation (11), M_{jk}^h is the mass and inertia matrix of the ship, ξ_k , $\dot{\xi}_k$ and $\ddot{\xi}_k$ are the time-domain displacement, velocity and acceleration vectors respectively, $A_{jk}^h(\infty)$ and $B_{jk}^h(\infty)$ are the infinite frequency added mass and damping coefficients, K_{jk}^h are the memory functions for related motion modes, C_{jk}^h is the constant restoring force matrix, $F_j^I(t)$ and $F_j^D(t)$ are the incident and diffraction forces in the time

domain. The superscript h indicates that all hydrodynamic forces are calculated with respect to the steady translating hydrodynamic frame in the time-domain simulations.
In LARes :L2 the non-linear incoming wave pressure and non-linear hydrostatic pressure are calculated as (Van't Veer et al., 2009):

$$P_{FK} = \begin{cases} \rho g \zeta_a \left(1 - \frac{z}{\zeta_a}\right) & 0 < z \leq \zeta_a \\ \rho g \zeta_a e^{kz} & z \leq 0 \end{cases} \tag{12}$$

$$P_{hydrostatic} = \begin{cases} 0 & 0 < z \leq \zeta_a \\ \rho g z & z \leq 0 \end{cases} \tag{13}$$

where ζ_a is the incident wave height, ρ is the water density and g is the gravity acceleration.
Memory functions, which account for the frequency dependant part of the hydrodynamic radiation force, are calculated from the damping curve provided by the 3-D linear frequency domain Mhydro code. Memory functions only depend on the forward speed and mean underwater part of the hull. Smoothness of the damping curve is crucial for the robustness of the memory functions. Spikes in the damping curve result in inconsistencies in the memory functions and will produce inaccurate damping forces in the main motion equation. (Ogilvie, 1964) showed that frequency domain damping forces can be related to retardation functions by Fourier transform:

$$K_{jk}^{h}(t) = \frac{2}{\pi} \int_0^\infty \left[B_{jk}^{h}(\omega_e) - B_{jk}^{h}(\infty)\right] \cos(\omega_e \tau) d\omega_e \qquad \text{j,k=3\&5} \tag{14}$$

where B_{jk}^{h} (j,k=3&5) and ω_e are the heave and pitch damping coefficients and encounter frequency respectively.
In time domain analysis the length of the retardation functions is very important where the retardation function needs to approach zero near the defined truncation time. After the end of the truncation time, radiation force components must converge to zero when convoluted with non-zero velocity history. In the current S-175 containership hull, the length of the retardation functions is applied to be 50 seconds due to the motions initiated by an impulse die out after that period of time.
In this study nonlinear ship accelerations are solved in the hydrodynamic coordinate system and velocity and displacement are derived using numerical integration via Runge-Kutta equations. Accelerations of the ship can be represented on the hydrodynamic frame axis and the equations can be solved using the same system unless the pitch angle is more than 8-10 degrees (Fonseca and Soares, 1998).

3 RESULTS

The S-175 container ship has been investigated in experimental and numerical studies since 80's. Vast amount of data provides a good basis for validation and comparison purposes. The main particulars of the S-175 container ship are provided below in Table 1.

Table 1: Main particulars of S-175 Containership

Parameters		Values
L_{pp}	[m]	175.0
Beam amidships	[m]	25.4
Draught amidships	[m]	9.5
Depth amidships	[m]	15.4
Displacement	[tonnes]	24668
LCG from the midship	[m]	-2.557
Pitch radius of gyration	[m]	43.75

3.1 Validation

For validation purposes, the in-house developed programmes Mhydro and LARes L2 has been applied to the simulation of motions of the S-175 containership. This section contains the linear RAO comparison of the S175 ship with the experiments performed by Fonseca and Soares (2004). Non-linear time-domain ship motion simulations are verified with the linear time-domain simulations and with the experiments in small amplitude waves and are shown in the Figure 2. It can be seen from the linear RAO's that the linear and non-linear time-domain responses are nearly identical to each other in small amplitude waves and they have a well agreement with the experiments. Around the resonant frequency, an over-estimation of the heave and pitch response is observed and the reason for that is attributed to the lack of damping forces which is originated from the frequency domain BVP solution.

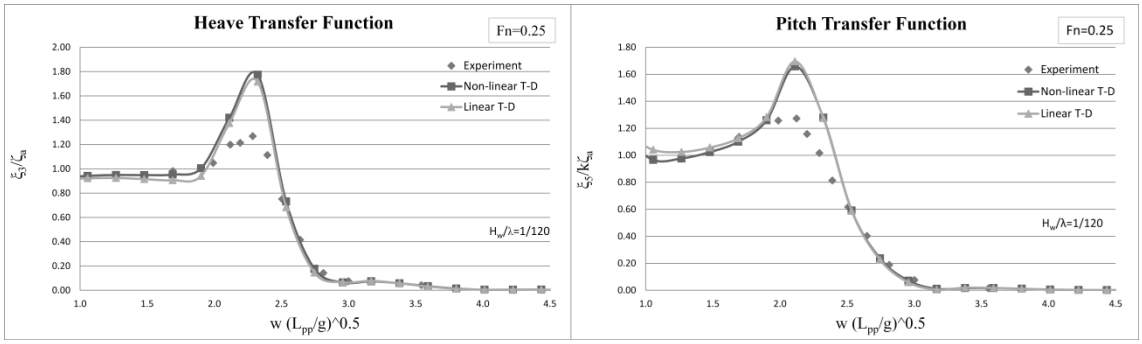

Figure 2: Heave and pitch RAOs, S-175 ship, head seas, Fn=0.25

3.2 Analysis and discussion

In order to investigate the motion responses in large amplitude waves, S-175 container ship is tested with respect to the increasing wave slope in regular waves in head seas. Fourier analysis is applied to the steady state part of time histories and in the current study only the first harmonics of the motion responses are investigated. In the Figure 3, the variation of the non-dimensional heave and pitch transfer functions at three forward speed cases (Fn=0.20, 0.25, 0.275) at the resonant frequency (λ/L=1.2) are compared with the experimental study which was performed by ITTC (2010) with respect to the increasing wave slope. Around the resonant frequencies ship motions and loads are amplified therefore the difference in the motion estimations between the linear and non-linear methods are observed to be at the highest level. It can be observed from the Figure 3 that the overall agreement of the LARes L2 program is well with the experiments. LARes L2 program followed the descending trend of the heave and pitch responses in the experimental results with the increasing wave slope. It is also observed that the LARes L2 program provides the best agreement with the experiments at the forward speed of Fn=0.20 when compared to the higher forward speed cases. The reason for this is attributed to the m-terms (gradients of steady velocities in the normal directions) influence in the modelling of the forward speed effects (Kim and Shin, 2007). In the present study, uniform flow approach is into account in order to simplify the m_j terms contribution in the BVP. Therefore, the order of the forward speed correction due to the m-terms contribution is increased with the increase in the forward speed. Fn=0.25 and 0.275 cases pitch response agreed better with the experiments than the heave responses. The reason for this is attributed to the damping coefficients in the BVP solution. Heave damping coefficients need to be augmented with empirical formulations in order to provide closer results to the experiments.

In the Figure 4, relative comparison of the non-dimensional heave and pitch transfer functions are performed at four different forward speed cases (Fn=0.15, 0.20, 0.25, 0.275) and around resonant frequencies, λ/L=1.0, 1.2, 1.4, w.r.t. the increasing wave slope. At the first sight, it is hard to make a general conclusion about the heave and pitch motion responses at different wave length to ship length ratios in different forward speed cases. However, at the wave length to ship length ratios of λ/L=1.2 and 1.4 heave and pitch responses show a descending trend with respect to the increasing wave slope. At the shortest wave length case, λ/L=1.0, heave

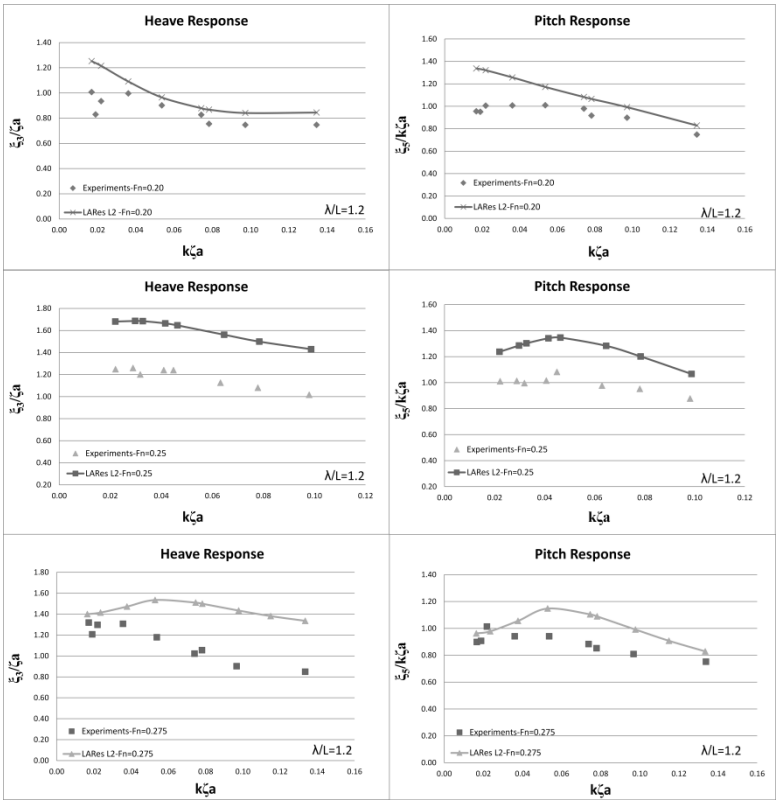

Figure 3: Comparison of heave and pitch transfer functions with experiments w.r.t. wave steepness, S-175 ship, head seas, Fn=0.20, 0.25, 0.275, λ/L=1.2

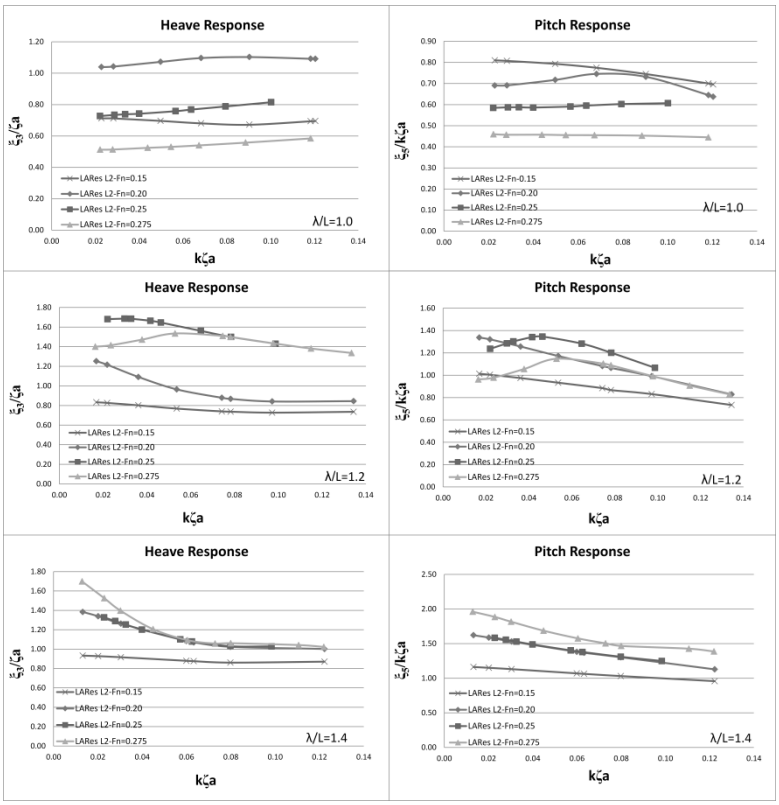

Figure 4: Comparison of heave and pitch transfer functions w.r.t. wave steepness, S-175 ship, head seas, Fn=0.15, 0.20, 0.25, 0.275, λ/L=1.0, 1.2, 1.4.

responses show an ascending trend with the increasing wave slope whilst at the same case pitch motions show either a constant or descending trend. In the heave responses, Fn=0.15 forward speed showed the least sensitivity with the increasing wave slope, but higher forward speed cases showed a higher sensitivity which resulted in a high descending slope. It is observed that at the shortest wave case the heave results of Fn=0.25 and 0.275 have a large difference whilst when the wave length is increased this difference is vanished. The forward speed Fn=0.20 showed the highest nonlinearity with the increasing wave slope. The tests revealed that, around the resonant frequency, heave and pitch responses are not directly proportional to the forward speed effects which mean that when the forward speed is increased it does not always cause an increase in the heave and pitch responses. This finding is completely related to the use of the EFS method in the BVP solution. It is a common phenomenon that when the AFS method is used in the BVP solution, it causes an increase in the heave and pitch responses around the resonance frequency with the increase in forward speed. In the pitch responses, especially at the wave length to ship length ratio of λ/L=1.2 and 1.4, responses show a steep descending trend with the increase in the wave slope. Again, this is caused by the non-linear F-K and restoring forces applied in the time domain calculations. At λ/L=1.0 ratio only the Fn=0.15 and 0.20 cases show a slight decrease in pitch responses whilst Fn=0.25 and 0.275 cases show a constant trend with the increasing wave slope. The pitch response difference between the Fn=0.25 and 0.275 cases are found to be at the highest level at the λ/L=1.0 case in which they showed a constant trend w.r.t the wave slope. However, at comparatively longer wave length cases, λ/L=1.2 and 1.4, Fn=0.25 and 0.275 speed cases showed a highly nonlinear behaviour with the increasing wave slope whilst they are observed to be getting closer to each other in large amplitude waves.

CONCLUSIONS

This paper presented a 3D nonlinear time domain method in order to investigate the forward speed effects in large amplitude waves. In order to take into account the forward speed influence a novel Rankine source method which was originally proposed by Yuan (2014) is used and the frequency domain results are post-processed using the LARes L2 (Hizir, 2015) time-domain programme. The present study is based on the Cummins (1962) theory, which takes into account the nonlinear F-K and restoring forces whilst the radiation and diffraction forces are kept as linear. It is observed that the non-dimensional heave and pitch responses agreed well with the experiments while they were observed to be following the experimental trends with the increasing wave slope. At the Fn=0.20 speed and at λ/L=1.2, numerical results agreed the best with the experiments and showed a highly non-linear behaviour with the increasing wave slope.All forward speed cases are relatively compared to each other and it was observed that heave and pitch responses are not linearly proportional to the increase in the forward speed. The reason for this is attributed to the use of the EFS method in the BVP solution. In most of the cases, except the λ/L=1.0 case, heave and pitch responses showed a descending trend with the increasing wave slope. The decrease in heave and pitch responses with the increasing wave slope is attributed to the non-linearity in the F-K and restoring forces.

ACKNOWLEDGEMENTS

The work presented in this paper is supported by the Lloyd's Register (LR) group that support a three year project on large amplitude waves. The authors are thankful for the support of the LR group. The LR group shall not in any way be responsible for the use of any knowledge, information or data that presented in the paper.

REFERENCES

Ba, M., Guilbaud, M. (1995). A Fast Method of Evaluation for the Translating and Pulsating Green's Function *Ship Technology Research*, **42** (2), 68-80.

Bruzzone, D., Gironi, C., Grasso, A., (2011). Nonlinear effects on motions and loads using an iterative time-frequency solver, International Journal of Naval Architecture and Ocean Engineering, p. 20.

Chang, M., (1977). *Computations of three-dimensional ship motions with forward speed*, 2nd Conference on Numerical Ship Hydrodynamics, pp. 124-135.

Chapchap, A., Ahmed, F., Hudson, D., Temarel, P., Hirdaris, S. (2011). The influence of forward speed and nonlinearities on the dynamic behaviour of a container ship in regular waves. *Trans. RINA*, **153** (2), 137-148.

Cummins, W.E. (1962). The impulse response function and ship motions. *Ship Technology Research*, **9**, 101-109.

Das, S., Cheung, K.F. (2012a). Hydroelasticity of marine vessels advancing in a seaway. *Journal of Fluids and Structures*, **34**, 271-290.

Das, S., Cheung, K.F. (2012c). Scattered waves and motions of marine vessels advancing in a seaway. *Wave Motion*, **49** (1), 181-197.

Fonseca, N., Soares, C.G. (1998). Time-domain analysis of large-amplitude vertical ship motions and wave Loads. *Journal of Ship Research*, **42** (2), 139-153.

Fonseca, N., Soares, C.G. (2004). Experimental investigation of the nonlinear effects on the vertical motions and loads of a containership in regular waves. *Journal of Ship Research*, **48** (2), 118-147.

Hizir, O.G., (2015). *Three Dimensional Time Domain Simulation of Ship Motions and Loads in Large Amplitude Waves*, Naval Architecture, Ocean and Marine Engineering. University of Strathclyde, Glasgow.

Inglis, R., Price, W. (1981a). The influence of speed dependent boundary condition in three-dimensional ship motion problems. *Int. Shipbuilding Progress*, **28** (318), 22-29.

Inglis, R., Price, W. (1981b). A three-dimensional ship motion theory: comparison between theoretical predictions and experimental data of the hydrodynamic coefficients with forward speed. *Trans. RINA*, **124**, 141-157.

ISSC, (2009). *17th ISSC Committee 1.2 Load-Technical report*, Seoul, Korea.

ITTC, (2010). *ITTC Workshop on Seakeeping*, *in: (ed.), i.Y.K. (Ed.)*, ITTC Towing Tank Conference, Seoul, Korea.

Jensen, G., Mi, Z.X., Söding, H., (1986). *Rankine source methods for numerical solutions of steady wave resistance problem*, Proceedings of 16th Symposium on Naval Hydrodynamics, Berkeley, pp. 575-582.

Kim, B., Shin, Y.-S. (2007). Steady flow approximations in three-dimensional ship motion calculation. *Journal of Ship Research*, **51** (3), 229-249.

Kring, D.C., (1994). *Time domain ship motions by a three-dimensional Rankine panel method*, PhD Thesis. MIT.

Nakos, D.E., (1990). *Ship wave patterns and motions by a three dimensional Rankine panel method*, PhD Thesis. MIT.

Nakos, D.E., Sclavounos, P.D. (1990). Steady and unsteady ship wave patterns. *Journal of Fluid Mechanics*, **215**, 263-288.

Ogilvie, T., (1964). *Recent Progress Toward the Understanding and Prediction of Ship Motions*, 5th Symp. on Naval Hydrodynamics. National Academy Press, Bergen, Norway.

Scalvounos, P.D., Nakos, D.E., (1988). *Stability analysis of panel methods for free surface flows with forward speed*, 17th Symposium on Naval Hydrodynamics, Den Hague, Nederland.

Song, M.-J., Kim, K.H., Kim, Y. (2011). Numerical analysis and validation of weakly nonlinear ship motions and structural loads on a modern containership. *Ocean Engineering*, **38** (1), 77-87.

Tuitman, J., (2010). *Hydro-elastic response of ship structures to slamming induced whipping.* Delft Technical University.

Van't Veer, A.P., Van Daalen, E., Willemstein, I.T., (2009). *PRETTI v1.5 Theory Manual*.

Watanabe, I., Guedes Soares, C. (1999). Comparative study on the time-domain analysis of non-linear ship motions and loads. *Marine Structures*, **12** (3), 153-170.

Wu, G., Taylor, R.E. (1990). The hydrodynamic force on an oscillating ship with low forward speed. *Journal of Fluid Mechanics*, **211**, 333-353.

Yuan, Z.-M., Incecik, A., Jia, L. (2014). A new radiation condition for ships travelling with very low forward speed. *Ocean Engineering*, **88** (0), 298-309.